Available online at www.sciencedirect.com
SCIENCE DIRECT®
Journal of the European Ceramic Society 25 (2005) 1565–1573
www.elsevier.com/locate/jeurceramsoc

Influence of the co-precipitation temperature on phase evolution in yttrium-aluminium oxide materials

Paola Palmero[a,*], Claude Esnouf[b], Laura Montanaro[a], Gilbert Fantozzi[b]

[a] *Department of Materials Science and Chemical Engineering, Politecnico di Torino, Corso Duca degli Abruzzi, 24, 10129 Turin, Italy*
[b] *Groupe d'Etude de Métallurgie Physique et de Physique des Matériaux, INSA de Lyon, Villeurbanne, France*

Received 10 March 2004; received in revised form 6 May 2004; accepted 23 May 2004
Available online 13 August 2004

Abstract

Yttrium-aluminium garnet (YAG) powders were synthesized using a reverse-strike precipitation, by adding an aqueous solution of yttrium and aluminium chlorides to dilute ammonia while monitoring the pH to a constant value of 9. After precipitation, the gelly product was washed with dilute ammonia and absolute ethanol for avoiding hard agglomeration during drying. Precipitation and washing procedures were performed at three different temperatures, namely at 5, 25 and 60 °C. After drying, the powders were characterized by DTA/TG simultaneous analysis and then calcined at different temperatures and times. Phase evolution was investigated by X-ray analysis; the evolution of crystallites formation and growth as a function of the temperature was followed by TEM observations. In this paper, a relevant influence of the co-precipitation temperature on the phases appearance, crystallisation path and final homogeneity of these powders was demonstrated. Pure YAG was yielded starting from powder synthesized at low temperature, whereas the precipitation performed at 60 °C leaded to monoclinic $Y_4Al_2O_9$ appearance near YAG.

Keywords: YAG; Sol–gel processes; X-ray methods; Electron microscopy; Grain growth

1. Introduction

Yttrium-aluminium garnet (YAG)–alumina composites are promising materials for optical, electronic and structural applications.[1,2] In order to reduce the crystallization temperature, improve the phases purity of the final product and reach a highly homogeneous distribution of the two phases in the composite material, several types of wet chemical methods[2–7] have been already developed and successfully used for powder processing. Although a lot of investigations on pure alumina preparation have underlined the strong influence of some process parameters (temperature, pH, rate of addition and nature of the precipitation agent)[8–12] on the phase evolution and on the properties of the synthesized alumina, when wet chemical syntheses and particularly precipitation are used, similar studies on pure YAG are lacking in the literature, even if many have been recently addressed to the synthesis features.[13–20] In this work YAG powders have been synthesized by using reverse-strike precipitation[6,7,14,17–20] (i.e., adding an aqueous Y and Al salts solution to the precipitant solution) which has the advantage to assure a higher cations homogeneity in the precipitate precursor in the case of multi-cation materials.[20] The influence of the final pH value cannot be significantly investigated since a complete precipitation of both Y and Al hydroxides is reached at pH of around 9.[14,17,19,20] Therefore, this study was focused on the precipitation temperature, which has demonstrated to be a crucial parameter in the production of pure alumina materials, and on its influence on the YAG phase evolution during the subsequent thermal treatments, above all considering the possible nucleation of secondary phases[21] such as orthorhombic perovskite (YAP, $YAlO_3$), hexagonal phase (h-$YAlO_3$), cubic $YAlO_3$ having a garnet structure $Y_3AlY(AlO_4)_3$ and monoclinic YAM ($Y_4Al_2O_9$), near the 3:5 molar ratio garnet-type compound (YAG, $Y_3Al_5O_{12}$).

* Corresponding author. Fax: +39 011 5644699.
E-mail address: paola.palmero@polito.it (P. Palmero).

0955-2219/$ – see front matter © 2004 Elsevier Ltd. All rights reserved.
doi:10.1016/j.jeurceramsoc.2004.05.027

2. Experimental procedure

In a laboratory equipment, a mixed chloride solution containing Y and Al ions in molar ratio 3:5 was added to 8 M ammonia solution while keeping a constant pH value of 9 by adding extra-ammonia solution, under continuous monitoring by a pH-meter to allow very small pH fluctuations (±0.2 pH units). After that, the gelatinous precipitate was washed for four times using dilute ammonia at a pH of 9 and finally twice with absolute ethanol for avoiding hard agglomeration during drying,[14] performed in oven at 60 °C for 48 h. The precipitation and the following washing procedures were carried out at three different temperatures, namely at 5, 25 and 60 °C. The precipitation and washing equipment was kept at 5 ± 1 °C by immersion in a refrigerating bath, whereas in the case of the higher temperatures all the operations were performed in a thermostatic bath. These samples will be labelled from now on YAG5, YAG25 and YAG60, respectively. After drying, the powders were characterised by DTA/TG simultaneous analysis (Netzsch STA 409C) and, on the ground of such results, pre-treated at different temperatures and times: the phase evolution was studied by X-ray diffraction (XRD, Philips PW 1710) and the crystallites formation and growth was followed by TEM (Jeol 200 CX) observations.

3. Results and discussion

After drying at 60 °C, YAG5 and YAG25 powders were completely amorphous, whereas traces of bayerite were detected in YAG60 by XRD. These results are in partial agreement with the studies performed on pure alumina,[8,9,12] in which highly crystalline precipitates are formed at higher (precipitation or hydrolysis) temperatures. Well-crystallised $Al(OH)_3$ (bayerite) was also detected in a YAG co-precipitated from nitrates solutions at room temperature using the reverse-strike technique,[19] whereas amorphous starting powders were obtained using other routes.[13,17,20]

In Fig. 1a–c the DTA/TG curves of the three YAG powders are reported. All the samples present a significant weight loss in the 100–400 °C range, associated to an important endothermic peak at about 230 °C for all the powders. This temperatures range is compatible to the dehydration of aluminium mono and trihydrates[10] and of yttrium hydroxides;[22] however, XRD diffraction patterns performed on powders pre-treated at various temperatures from 200 up to 450 °C showed that these mass changes and thermal effects cannot be imputed to the dehydration of crystalline compounds. Therefore, they can be due to the progressive stripping of OH groups from the amorphous precipitate.

The three samples also differ in the higher temperature regime. An exotherm at about 902 °C was observed on the sample YAG5; an exotherm at about 900 °C is also presented by the sample YAG25 followed by a broad and slightly intense effect at higher temperature. Finally, a very sharp peak located at about 904 °C is associated to a larger and weaker

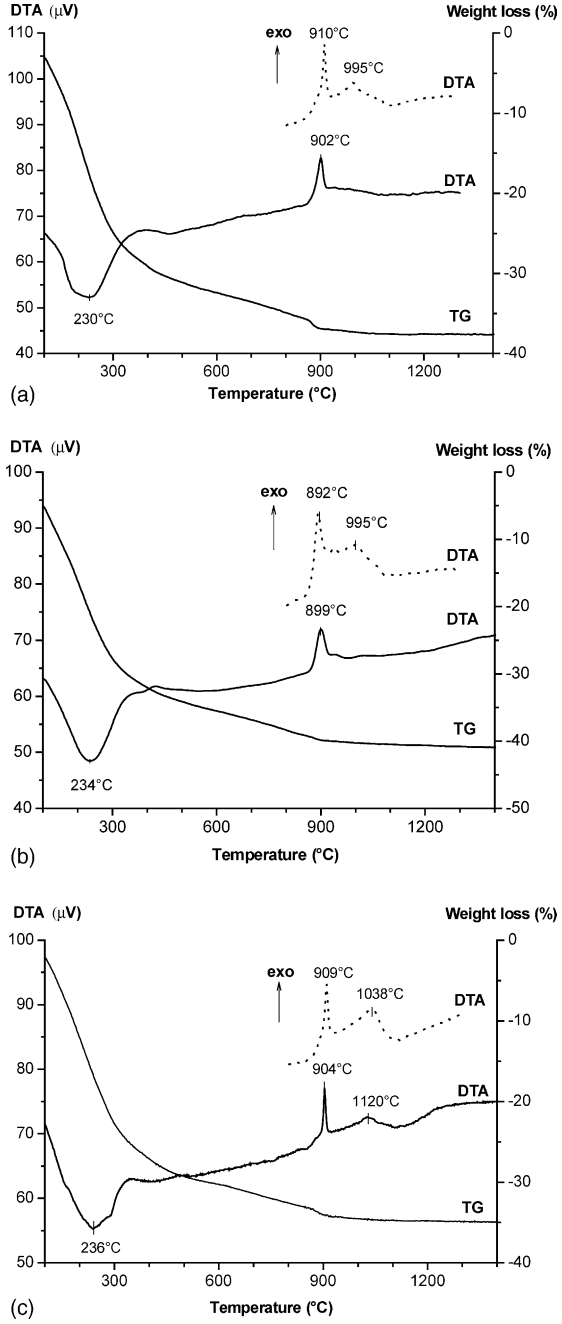

Fig. 1. DTA/TG curves of the dried powders synthesised at (a) 5 °C; (b) 25 °C; and (c) 60 °C (solid curves) and pre-treated at 800 °C (dotted curves).

peak at 1020 °C in sample YAG60. Dotted curves reported in Fig. 1a–c, represent the temperature range of crystallization of the DTA curves for the three samples pre-treated at 800 °C. The pre-treatment allows to better distinguish the thermal effects associated to the crystalline phases appearance. For YAG5 (dotted curve in Fig. 1a) the peak maximum is located at 910 °C and an exothermal peak can be also clearly detected at about 995 °C. Also in the case of YAG25 the pre-treatment allowed to better evidence the broad exotherm at about 995 °C (dotted curve in Fig. 1b). For YAG60 the peak maximum is located at about 910 °C followed by a broad and

intense exotherm at about 1040 °C (dotted curve in Fig. 1c). A small intermediate peak at about 950 °C appears in the curves of YAG5 and YAG25, but XRD analysis of samples calcined at this temperature did not allow to relate it to a new phase appearance.

All these exothermic peaks are associated to the crystallisation of yttrium aluminates, as previously proposed by Yamaguchi et al.[16] Particularly, the sharp peak at about 900 °C can be associated to the crystallisation of h-$YAlO_3$, whereas the broader and less intense peak at higher temperature can be due to the transition from the hexagonal phase to the 3:5 garnet-type YAG. Such phase evolution was also confirmed by XRD, as described below.

A different phase evolution was observed as a function of the synthesis temperature, as shown by a systematic investigation performed by XRD on powders calcined at different temperatures (chosen on the ground of the above DTA/TG curves) and times.

In Fig. 2a–c the XRD patterns of the three materials are compared after calcination at 800, 850, 915 and 1100 °C with a heating and cooling rate of 10 °C/min and a zero-time soaking at the maximum temperature. Even if the whole patterns from 5 to 70° 2θ have been considered for discussion, only the 2θ range between 31 and 35° of each XRD pattern is reported in these figures, since the crystallisation of YAG and secondary phases can be more easily followed by enlarging this portion of the pattern. In fact, at 33.297° 2θ the more intense peak of YAG appears (d = 2.6886 Å, planes {4 2 0} JCPDS file no. 82-0575), whereas those of the two phases, h-$YAlO_3$ and YAP, are at 32.832° 2θ (d = 2.7257 Å, planes {1 0 2}, JCPDS file no. 74-1334) and at 34.236° 2θ (d = 2.6170 Å, planes {1 2 1}, JCPDS file no. 70-1677), respectively. No evidence of the formation of YAP as well as of cubic $YAlO_3$ was found during these analyses.

The phase evolution clearly appears strongly dependent from the powder synthesis temperature. In fact, in sample YAG5, crystallization starts at about 915 °C with the simultaneous appearance of the peaks attributed to h-$YAlO_3$ and YAG. The more intense YAG peak is higher than the corresponding one of the hexagonal phase.

Also in the case of YAG25, the same phases are yielded at 915 °C, and traces of both can be already detected at 850 °C. However, in this material, the intensities of the principal peaks of h-$YAlO_3$ and YAG are quite the same. The increase of the hexagonal phase content is also put in evidence by the more clear appearance of its secondary peak located at 34.062° 2θ which corresponds to the {0 0 4} planes.

YAG60 crystallises at 915 °C yielding only the h-$YAlO_3$, and also in this case the starting of crystallisation can be detected after calcination at 850 °C.

After treatment at 1100 °C pure YAG is the only phase detected in YAG5 and YAG25, whereas it is the prevalent one in YAG60, since YAM phase is also yielded as explained below.

XRD characterization was then improved on differently calcined samples to go deeper in the comprehension of the phases evolution as a function of the synthesis temperature. In fact, if thermal treatments are performed at the same temperature but for different soaking times, other interesting features can be drawn out.

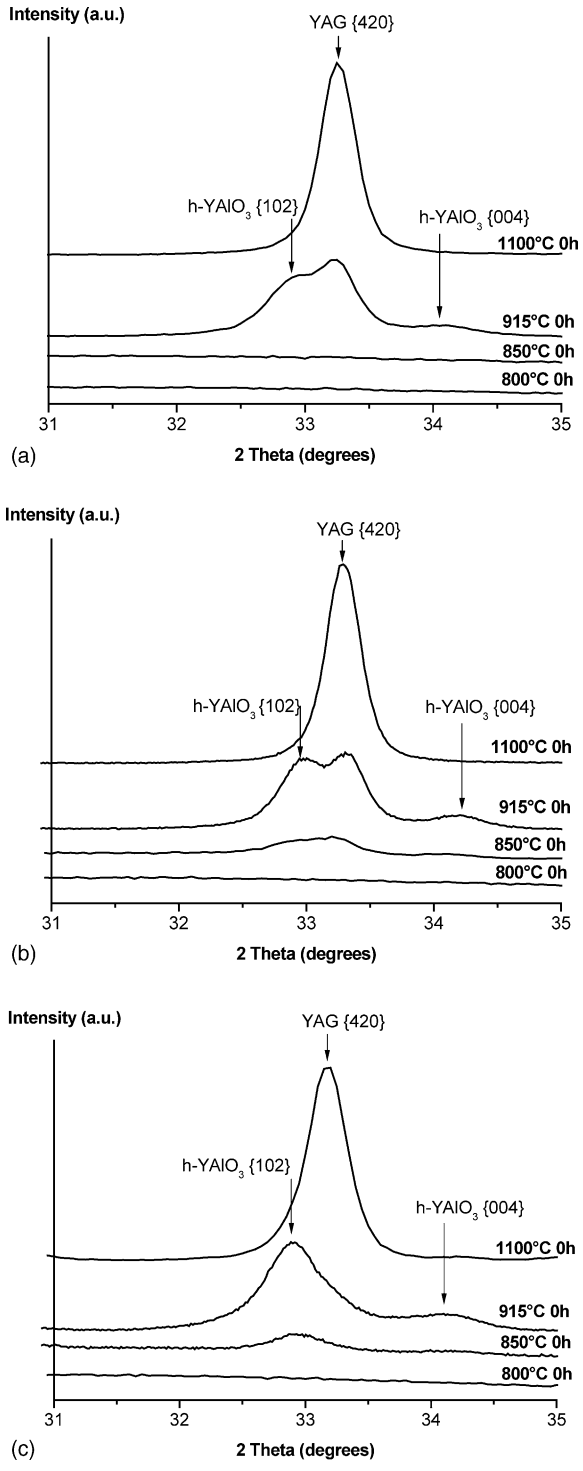

Fig. 2. XRD patterns of YAG synthesised and calcined at different temperatures: (a) YAG5; (b) YAG25; and (c) YAG60.

In Fig. 3a–c the above 2θ range of the XRD patterns performed after treatment at 850 °C for 0, 0.3, 0.5, 1, 2 and 4 h

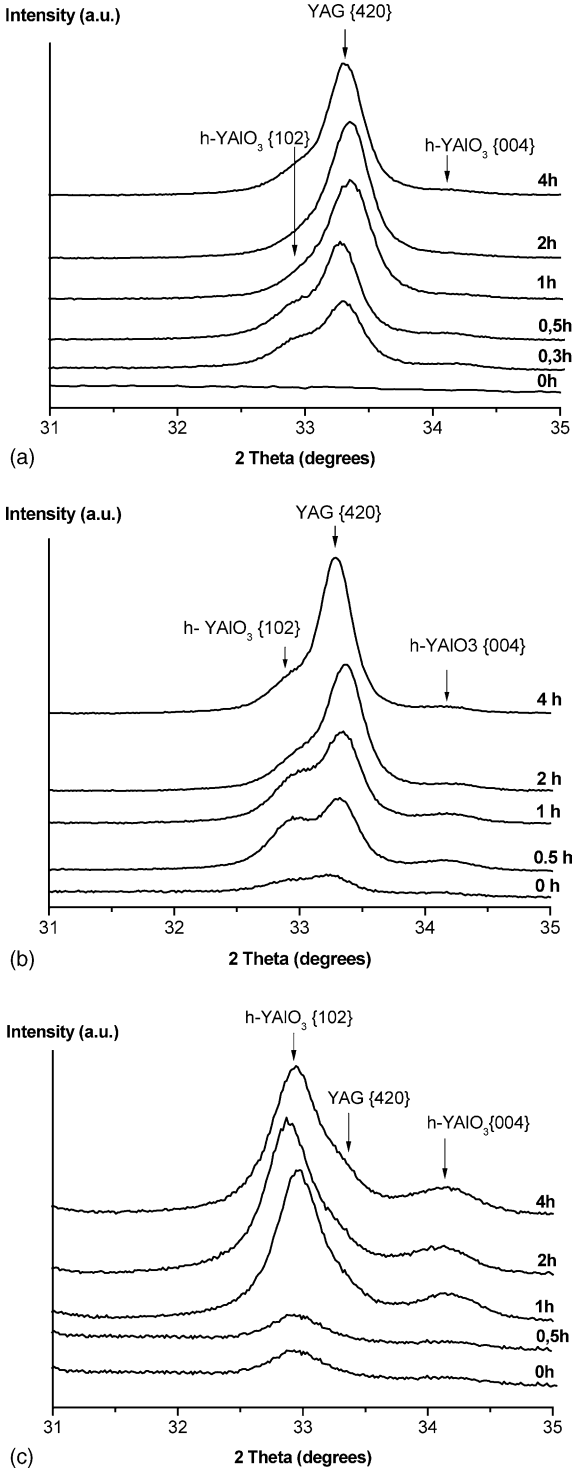

Fig. 3. XRD patterns of the YAG powders synthesised at different temperatures and calcined at 850 °C for different times: (a) YAG5; (b) YAG25; and (c) YAG60.

for sample YAG5 and for 0, 0.5, 1, 2 and 4 h for the other two powders are collected.

In the case of YAG5, the garnet starts to crystallise after about 15 min soaking at 850 °C and the intensities of the YAG peaks increase with increasing the soaking time (0.5 up to 4 h). At this temperature, even for long-time treatment, only traces of h-$YAlO_3$ were detected. Even if it is difficult to discriminate a clear behaviour by referring only to a phase present in traces, it seems that h-$YAlO_3$ is present after 0.3, 0.5 and 1 h, but its amount decreases progressively until it is undetectable after 2 h treatment. After 4 h a very small shoulder is detectable on the left size of the YAG peak, still imputable to h-$YAlO_3$ traces.

The YAG25 precipitate starts to crystallise at zero soaking time. When the sample is treated for longer times at 850 °C, the amount of YAG monotonically increases, whereas h-$YAlO_3$ yielded after short time calcination does not change significantly as a function of the soaking time. This behaviour was clearly observed by calcining the powder at 800 °C for 0, 0.5, 1, 2 and 4 h (Fig. 4a) or at 850 °C for 0, 0.5, 1, 2 and 4 h (Fig. 4b) and by plotting the peak intensities ($I_{\{420\}}$ for YAG and $I_{\{102\}}$ for h-$YAlO_3$) as a function of the treatment time. In Fig. 4c and d the same data are reported for YAG5 and YAG60, respectively, treated at 850 °C. In Fig. 4 the height of the symbols represents the data fluctuations evaluated from at least three different XRD pattern acquisitions. In Fig. 4b the amount of h-$YAlO_3$ reaches a maximum after 30 min; then, its amount decreases due to a partial conversion in the YAG phase. In Fig. 4c, $I_{\{102\}}$ of the hexagonal phase after 1 and 2 h of soaking time has not been plotted, since it is covered by the stronger $I_{\{420\}}$ YAG peak.

In the sample YAG60, h-$YAlO_3$ firstly crystallises at 850 °C even without a soaking step. This phase remains the only one present in the sample up to a 4 h treatment; after that, YAG traces were also detected.

In addition, some other thermal treatments were performed. For instance, if the powder YAG5 pre-treated at 850 °C for 2 h is re-heated up to 915 °C, for a soaking time of zero, the peaks of the hexagonal phase are no more detected and only an increase of the intensities of the YAG peaks was observed (Fig. 5, curve b). This behaviour is therefore in contrast with the phase evolution in an amorphous product continuously heated up to 915 °C (compare Fig. 2a and Fig. 5, curve a), in which both h-$YAlO_3$ and YAG were detected by XRD. Therefore, it can be reasonably assumed that when crystallisation happens starting from an amorphous product there is a competition in the appearance of these two phases, whereas if YAG crystallites are already formed during a lower temperature treatment (850 °C), nucleation of the metastable phase h-$YAlO_3$[21] is not favourite with respect of the growth of the pre-existing YAG crystals. This behaviour could be imputed to different nucleation and growth kinetics of these two phases and more details on the crystallization kinetic have been published elsewhere.[23] A similar treatment was not performed on YAG25 because in this case it was not possible to find a temperature lower than 1100 °C at which pure YAG is yielded. On the other hand, for YAG60, only the metastable phase h-$YAlO_3$ was present after treatment in that intermediate temperature range.

For concluding the XRD data discussion, YAG60 powders appeared a less homogeneous product than the other two. In

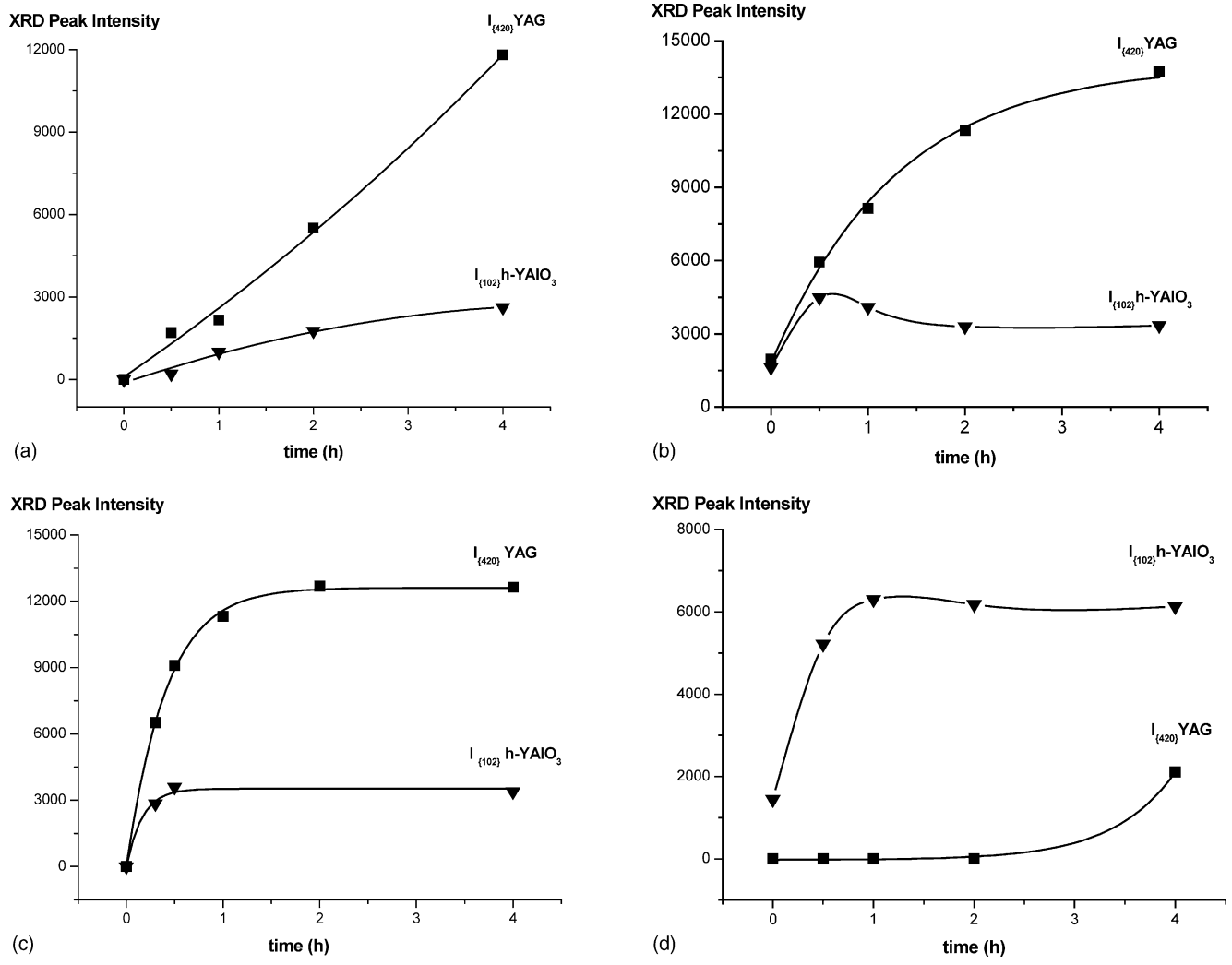

Fig. 4. Evolution of the intensities of the main XRD peak of the crystalline phases as a function of the calcinations temperature and time: (a) YAG25 at 800 °C; (b) YAG25 at 850 °C; (c) YAG5 at 850 °C; and (d) YAG60 at 850 °C.

fact, starting from 850 °C also traces of monoclinic phase (YAM, Y_4AlO_9) were yielded in this material. The amount of this secondary phase remains at a trace level up to the higher treatment temperature. A singular behaviour can be observed comparing the XRD patterns of YAG60 treated at 915, 1000 and 1100 °C for 0 h, and finally at 1350 °C for 0.5 h (Fig. 6). At the lowest temperatures, still traces of YAM are present, whereas its characteristic peaks strongly increased with increasing the calcination temperature, probably as a consequence of the disappearance of the hexagonal phase, no more detectable at 1100 °C. In Fig. 6 the XRD pattern of YAG25 calcined at 1350 °C for 0.5 h is shown for comparison. It clearly appears that YAM is completely absent in YAG25, since the YAM peak $\{2\,1\,1\}$ is no more detected and there is no contribution of YAM $\{-2\,2\,1\}$ to the YAG peak $\{4\,0\,0\}$. Therefore, YAG60 leads to a biphasic final product, in contrast with the other two powders, just synthesised at a different temperature, and the traces of bayerite in the dried product are probably a signal of a less homogeneous starting precipitate.

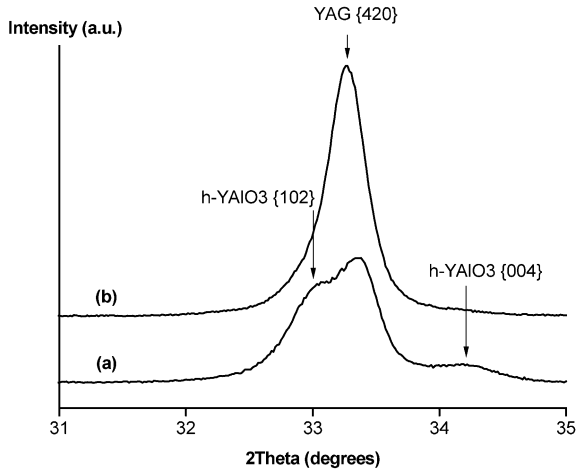

Fig. 5. XRD patterns of YAG5 obtained by calcinations at 915 °C starting from the amorphous precipitate, just dried at 105 °C (curve a), and from the powder pre-treated at 850 °C for 2 h (curve b).

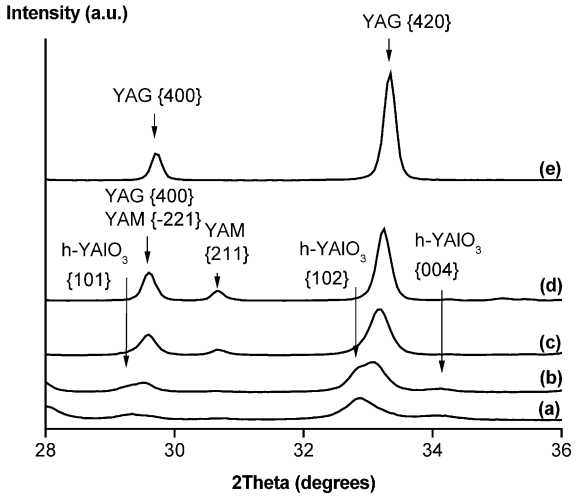

Fig. 6. XRD patterns of YAG60 powders calcined at (a) 915 °C; (b) 1000 °C; (c) 1100 °C for 0 h; (d) 1350 °C for 0.5 h and (e) YAG25 powder calcined at 1350 °C for 0.5 h.

On the contrary, the precipitation temperature does not significantly affect the evolution of the crystallites size of the three powders as a function of the calcinations temperature. A similar trend is in fact presented by the curves in Fig. 7 in which the crystallites mean size, estimated by a large number of determinations from TEM observations, are reported. Some of the images of this extensive TEM investigation are collected in Figs. 8–10 for YAG5, YAG25 and YAG60, respectively. In each figure, an insert with the corresponding diffraction pattern is shown. In Fig. 8a, YAG5 powder just dried at 60 °C is totally amorphous as confirmed by the diffraction pattern. In Fig. 8b, the TEM image of the same powder calcined at 915 °C is shown: the d_{hkl} values measured from the diffraction pattern performed on a large zone of the powder deposited on a carbon film, confirmed the simultaneous presence of both YAG and h-$YAlO_3$ phases. Finally, the TEM micrograph of the powder calcined at 1350 °C for 30 min (Fig. 8c) shows a well-crystallised, pure YAG, as confirmed by the experimental d_{hkl} values measured from the diffraction pattern.

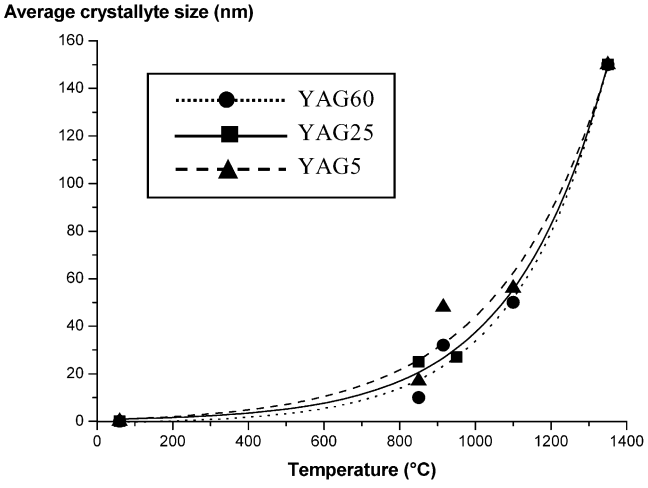

Fig. 7. Evolution of the crystallites size of the powders YAG5 (dashed line), YAG25 (solid line) and YAG60 (dotted lines), as determined by TEM observation.

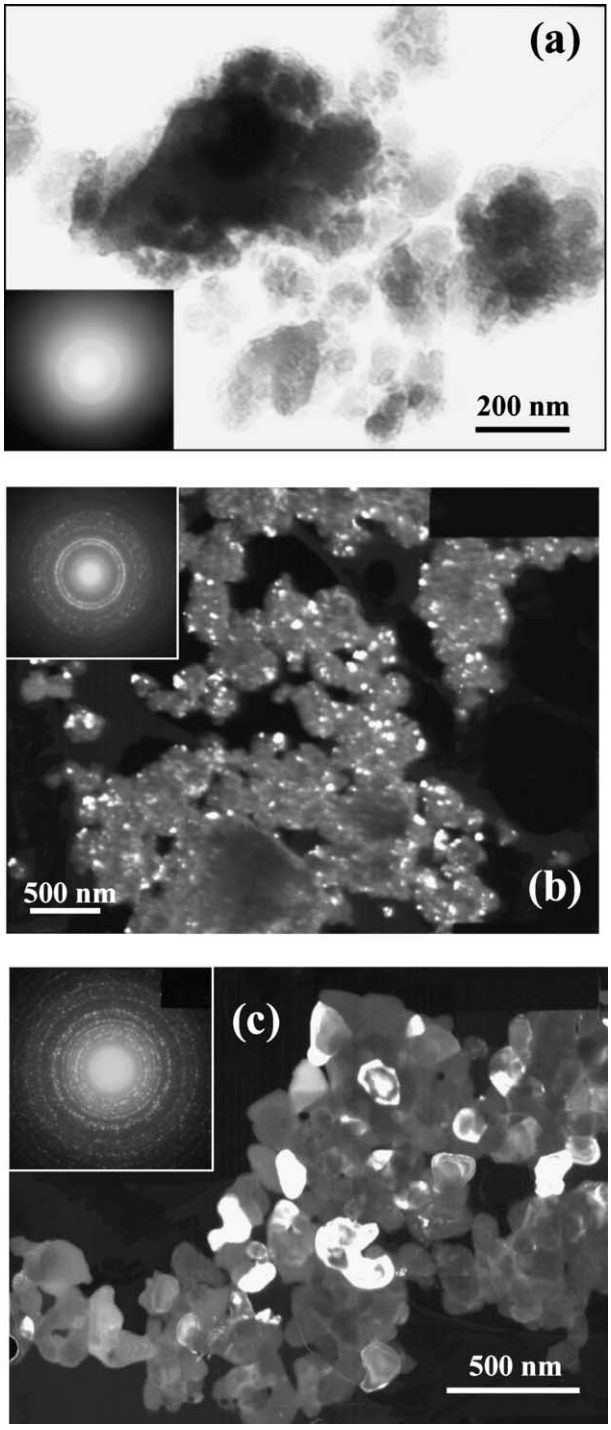

Fig. 8. TEM micrographs of: (a) YAG5 just dried at 60 °C (bright field), (b) pre-treated at 915 °C (dark field) and (c) at 1350 °C for 30 min (dark field).

In Fig. 9a, the 60 °C dried amorphous YAG25 powder is shown. Fig. 9b shows the same powder after pre-treatment at 950 °C, at which YAG is the predominant phase. Finally,

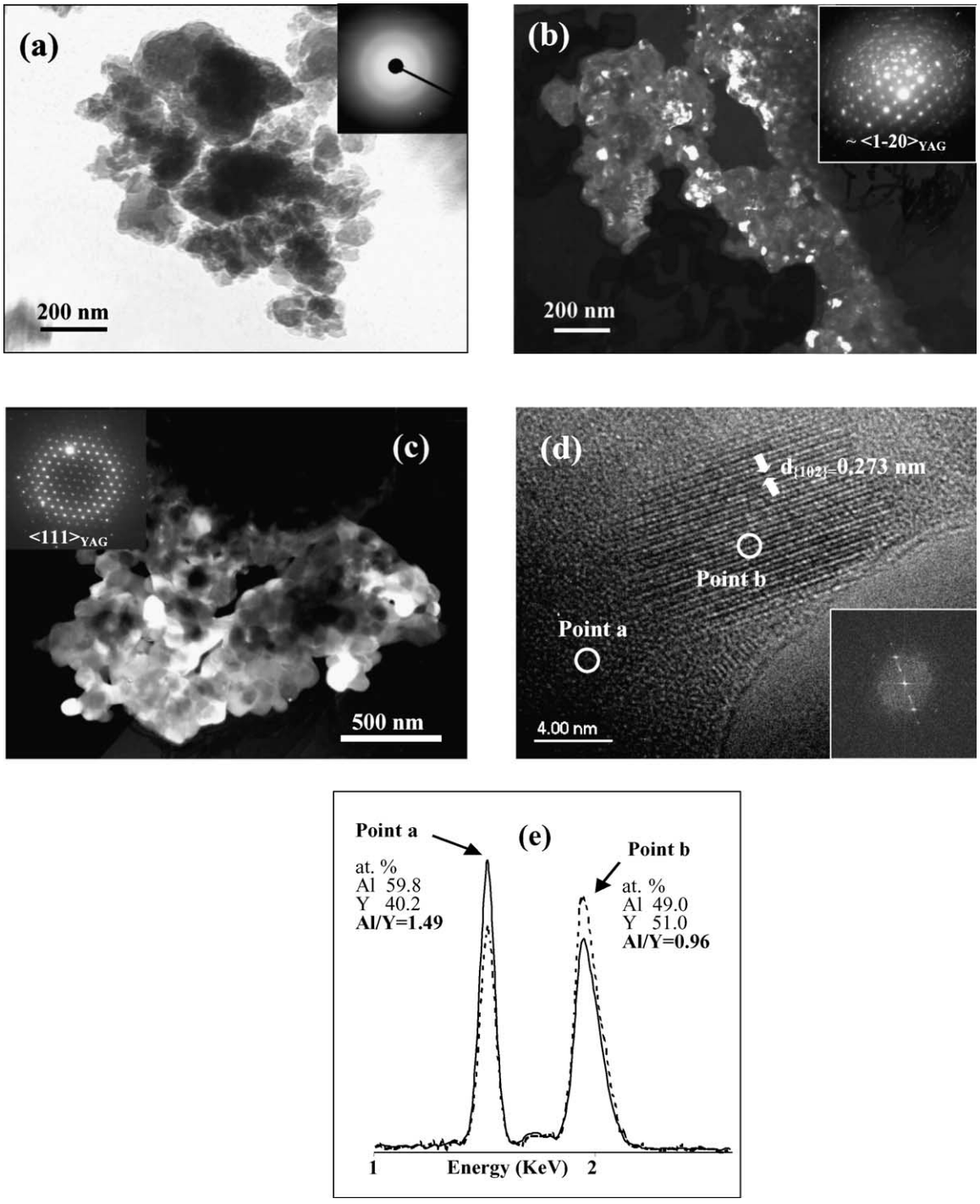

Fig. 9. TEM micrographs of (a) YAG25 just dried at 60 °C (bright field), (b) pre-treated at 950 °C (dark field) and (c) at 1350 °C for 30 min (dark field). (d) An high-resolution TEM image of YAG25 pre-treated at 850 °C is shown while in (e) the EDX peaks intensities of Y and Al determined on the crystallite and, as comparison, on the matrix, are represented.

when powder YAG25 is calcined at 1350 °C for 30 min (Fig. 9c), YAG is the only phase present. In the insert, the diffraction pattern obtained on a single YAG grain is reported. In Fig. 9d, the high-resolution TEM (Jeol 2010 FEG) image of YAG25 calcined at 850 °C shows the appearance of a very small crystallite from the amorphous matrix and the related Fast Fourier Transform is shown in the insert. From EDX analysis (Fig. 9e) performed on the crystallite and on the surrounding matrix, this crystallite was attributed to the h-$YAlO_3$ phase, as also confirmed by the experimentally measured distance of 0.273 nm between the lattice fringes associated to {1 0 2} lattice planes of the hexagonal phase.

In Fig. 10a and b, YAG60 powders just dried at 60 °C and after treatment at 915 °C are shown, respectively. The $d_{h\,k\,l}$

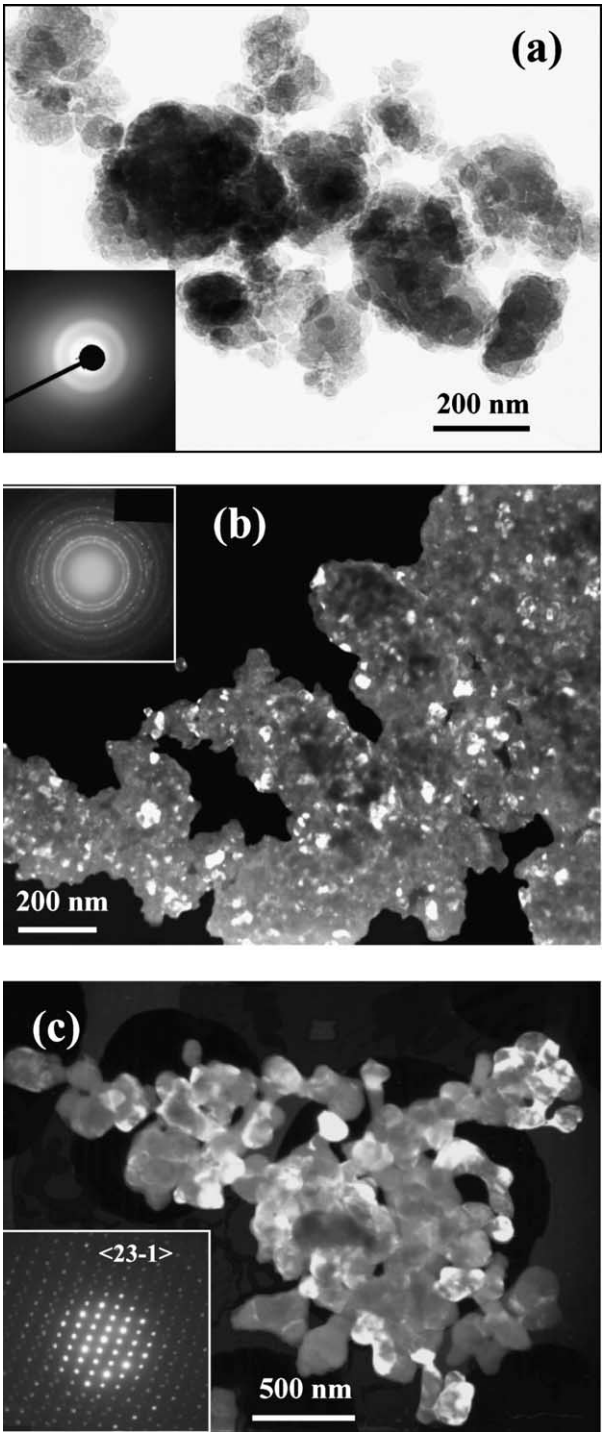

Fig. 10. TEM micrographs of (a) YAG60 just dried at 60 °C (bright field), (b) pre-treated at 915 °C (dark field) and (c) at 1350 °C for 30 min (dark field).

values estimated from the diffraction patterns performed on several crystallites confirmed a predominant presence of the hexagonal phase at 915 °C. In Fig. 10c, powder calcined at 1350 °C for 30 min is shown: YAG is the predominant phase and the diffraction pattern on a single YAG grain is included in the figure.

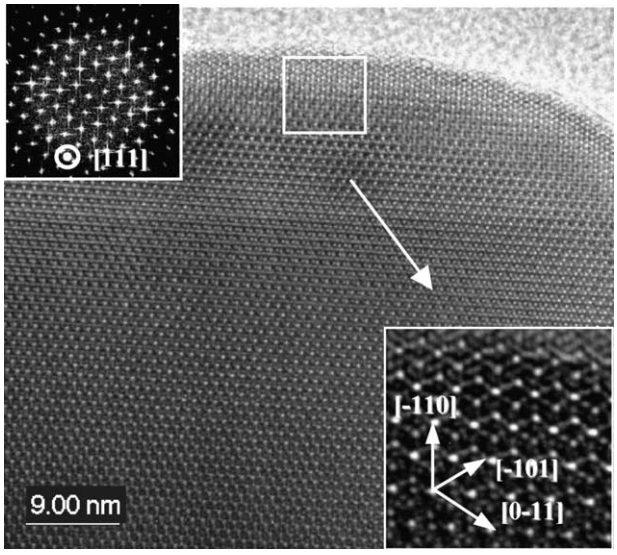

Fig. 11. High-resolution TEM image of a YAG25 grain, observed along the {1 1 1} zone axis, as confirmed by the Fast Fourier Transform included in the image. The atomic structure of YAG is better observed trough an higher magnitude image performed on a boundary zone of the grain, as shown in the insert.

In Fig. 11, a high-resolution TEM micrograph of YAG25 calcined at 1350 °C for 30 min is reported: pure YAG composition was confirmed by EDX analysis performed with a nanoscale probe. In the image the YAG atomic structure is observed along the {1 1 1} zone axis: the hexagonal projection of the cubic structure of YAG is better evidenced by the higher magnitude image, performed on a boundary zone of the grain (insert in Fig. 11). The atomic distances experimentally measured resulted to be in a very good agreement with the cell crystallographic parameter of the YAG phase.

4. Conclusions

From the above results the following conclusions can be drawn out:

(a) the synthesis of YAG powder performed at three different temperatures (5, 25, and 60 °C) by following the same precipitation procedure leads to products which mainly differ in terms of crystallisation temperature, phase evolution as a function of the heat treatment and soaking time and final homogeneity;
(b) also the starting crystallization temperature is affected by the synthesis temperature, since it is about 915 °C for YAG5 and 850 °C for the other two powders;
(c) during crystallization, YAG synthesised at 5 °C yielded higher amounts of YAG in all the investigated temperature and time range. YAG crystallised firstly and only traces of the metastable h-$YAlO_3$ were detected in the crystallization temperature range. In addition, if a sample in which YAG crystallites were already grown at very low

temperature was reheated, nucleation of the metastable h-$YAlO_3$ was no more favourite;

(d) YAG synthesised at 25 °C showed a competition between YAG and h-$YAlO_3$ crystallization in all the investigated temperature and time range;

(e) YAG synthesised at 60 °C firstly yielded h-$YAlO_3$ and YAG was formed only at 1100 °C;

(f) all the powders yielded pure YAG after calcination at 1100 °C; however, in the case of YAG60, the product was less homogeneous since bayerite traces were already detected in the amorphous powder and YAM traces progressively increased with calcinations temperature from 850 up to 1350 °C.

Acknowledgement

P. Palmero wishes to thank the Italian Ministry MIUR to have partially supported this research in the framework of the project “Internazionalizzazione del dottorato”.

References

1. French, J. D., Zhao, J., Harmer, M. P., Chan, H. M. and Miller, G. A., Creep of duplex microstructures. *J. Am. Ceram. Soc.*, 1994, **77**, 2857–2865.
2. Veith, M., Mathur, S., Kareiva, A., Jilavi, M., Zimmer, M. and Huch, V., Low temperature synthesis of nanocrystalline $Y_3Al_5O_{12}$ (YAG) and Ce-doped $Y_3Al_5O_{12}$ via different sol–gel methods. *J. Mater. Chem.*, 1999, **9**, 3069–3079.
3. Hay, R. S. and Matson, L. E., Alumina/yttrium aluminium garnet crystallographic orientation relationships and interphase boundaries: observations and interpretation by geometric criteria. *Acta Metall. Mater.*, 1991, **39**, 1981–1994.
4. Towata, A., Hwang, H. J., Yasuoka, M. and Sando, M., Fabrication of fine YAG-particulate-dispersed alumina fiber. *J. Am. Ceram. Soc.*, 1998, **81**, 2469–2472.
5. Schehl, M. and Torrecillas, R., Alumina nanocomposites from powder-alkoxides mixtures. *Acta Mater.*, 2002, **50**, 1125–1139.
6. Li, W. Q. and Gao, L., Processing, microstructure and mechanical properties of 25 vol% YAG–Al_2O_3 nanocomposites. *Nanostruct. Mater.*, 1999, **11**, 1073–1080.
7. Wang, H. and Gao, L., Preparation and microstructure of polycrystalline Al_2O_3–YAG composites. *Ceram. Int.*, 2001, **27**, 721–723.
8. Mathieu, M. V., *Contribution a L'etude des Gels D'alumine Désorganisée*. Ph.D. Thesis, University of Lyon, 1956.
9. Yoldas, B. E., Effect of variations in polymerized oxides on sintering and crystalline transformations. *J. Am. Ceram. Soc.*, 1982, **65**, 387–393.
10. Carel, A. B. and Cabbiness, D. K., Analysis of alumina by combined TG/X-ray diffraction. *Am. Ceram. Soc. Bull.*, 1985, **64**, 716–719.
11. Pierre, A. C. and Uhlmann, D. R., Gelation of aluminum hydroxide sols. *J. Am. Ceram. Soc.*, 1987, **70**, 28–32.
12. Song, K. C. and Chung, I. J., The structure formations of aluminum hydroxide gels under HCl and NH_4OH conditions. *J. Non-Cryst. Solids*, 1989, **108**, 37–44.
13. Gowda, G., Synthesis of yttrium aluminates by the sol–gel process. *J. Mater. Sci. Lett.*, 1986, **5**, 1029–1032.
14. Vrolijk, J. W., Willems, J. W. and Metselaar, R., Coprecipitation of yttrium and aluminum hydroxides for preparation of yttrium aluminum garnet. *J. Eur. Ceram. Soc.*, 1990, **6**, 47–51.
15. Veitch, C. D., Synthesis of polycrystalline yttrium iron garnet and yttrium aluminium garnet from organic precursor. *J. Mater. Sci.*, 1991, **26**, 6527–6532.
16. Yamaguchi, O., Takeoka, K., Hirota, K., Takano, H. and Hayashida, A., Formation of alkoxy-derived yttrium aluminium oxides. *J. Mater. Sci. Lett.*, 1992, **27**, 1261–1264.
17. Wang, H., Gao, L. and Niihara, K., Synthesis of nanoscaled yttrium aluminum garnet powder by the co-precipitation method. *Mat. Sci. Eng.*, 2000, **A288**, 1–4.
18. Apte, P., Burke, H. and Pickup, H., Synthesis of yttrium aluminum garnet by reverse strike precipitation. *J. Mater. Res.*, 1992, **7**, 706–711.
19. Li, W. Q. and Gao, L., Co-precipitation processed needle-like YAG dispersed in alumina powder. *Mater. Lett.*, 2001, **48**, 157–161.
20. Li, J. G., Ikegami, T., Lee, J. H., Mori, T. and Yajima, Y., Co-precipitation synthesis and sintering of yttrium aluminum garnet (YAG) powders: the effect of precipitant. *J. Eur. Ceram. Soc.*, 2000, **20**, 2395–2405.
21. Lo, J. R. and Tseng, T. Y., Phase development and activation energy of the Y_2O_3–Al_2O_3 system by a modified sol–gel process. *Mater. Chem. Phys.*, 1998, **56**, 56–62.
22. Koelher, E. K., Kuznetsov, A. K., Tikhonov, P. A. and Kravchinskaya, M. V., DTA and electrical conductivity studies of polymorphic transformations of solid solutions in the Y_2O_3–Pr_2O_{3+x} and HfO_2–PrO_2 (Tb_2O_3) systems. In *Thermal Analysis, Vol 1*, ed. I. Buzás. Institute for General and Analytical Chemistry, Technical University, Budapest, Hungary, 1975, pp. 391–399.
23. Palmero, P., Esnouf, C., Fantozzi, G. and Montanaro, L., Influence of the synthesis temperature on the crystallization path and kinetics of YAG powder. In *Proceedings of 28th International COCOA Beach Conference and Exposition of Advanced Ceramics and Composites*, in press.